Molybdenum Loading Effects on the Physico-Chemical Properties and Performance of Carbon Nanotubes Supported Alkalized MoS_2 Catalysts for Higher Alcohols Synthesis

Tavasoli, Ahmad*+; Karimi, Saba; Nikookar, Hamideh; Fadakar, Hamzeh
School of Chemistry, College of Science, University of Tehran, Tehran, I.R. IRAN

ABSTRACT: *An extensive study of Higher Alcohols Synthesis (HAS) from syngas using alkalized MoS_2 catalysts supported on Carbon Nanotubes (CNTs) is reported. Up to 30wt.% of Mo and 8wt.% K are added to the CNTs by impregnation method. The catalysts were characterized by different methods and the performance of the catalysts was assessed in a micro-reactor. TEM images showed that most of the metal particles were homogeneously distributed inside the tubes and the rest on the outer surface of the CNTs, with particle sizes in the range of 3 to 16 nm. Temperature Programmed Reduction (TPR) tests showed that increasing the amount of Mo decreased the first TPR peak from 518 to 503°C and increased the second TPR peak temperature from 782 to 825°C. The diffraction peaks representing the characteristic K-Mo-O phase (these species can enhance formation of higher alcohols) were observed in the XRD of catalysts. The catalyst with 20 wt.% Mo and 8 wt.% K showed the highest conversion. The total alcohol selectivity reached a maximum of 45.3 wt.% on the catalyst with 15 wt.% Mo. The catalyst with 15 wt.% Mo exhibited selectivity of 35.3 wt.% towards higher alcohols.*

KEY WORDS: *Higher Alcohols Synthesis (HAS), Molybdenum, Loading, Carbon nanotubes, Physicochemical properties, Activity, Selectivity.*

INTRODUCTION

Higher alcohols synthesis from syngas, an economically attractive method for making fuels and chemicals, is interested due to the enhancement of petroleum price, environmental concerns, and additive for gasoline to increase octane number [1]. There are four methods for making higher alcohols from syngas: (I) using modified catalysts for synthesis of methanol at high temperature and pressure [2, 3]; (II) using modified catalysts for synthesis of methanol at low temperature and pressure [4, 5]; (III) using promoted MoS_2 catalysts [6-8] and (IV) using Co-Cu catalysts [9]. Among them, MoS_2 are more attractive due to their excellent resistance to sulfur poisoning and high water–gas shift activity [10]. MoS_2 catalyst mainly produces hydrocarbons but, when it is promoted with alkali metals, it can produce alcohols [11, 12]. The function of alkali is to reduce the hydrogenation ability of alkyl species and increase

* To whom correspondence should be addressed.
+ E-mail: tavassolia@khayam.ut.ac.ir
1021-9986/13/1/ 9/$/2.90

the sites, active for formation of alcohols [13]. Metal oxides and Activated Carbon (AC) are used as support for MoS_2 catalysts for higher alcohols synthesis [2, 20]. The use of CNTs has been drawing attention, due to their flexibility as support in tailoring the catalyst properties to specific needs [16, 21-23]. Activated carbon has many advantages if utilized as HAS catalyst support, CNTs possess similar properties and in most cases outperform AC in this respect. Carbon nanotubes with unique properties such as uniform pore size distribution, meso and macro pore structure, inert surface properties, highly graphitized tube-walls, sp^2-C-constructed surfaces (i.e. carbon nanotube is constructed from carbon atoms with sp^2 hybrid among one unpaired electron on each atom and due to the π-electrons on its surfaces can interact better with metal atoms) and resistance to acidic and alkaline environments can play an important role in a large number of catalytic reactions. It is probable that using mesoporous structured carbon nanotubes improve the catalytic performance. It is expected that the catalytic performance of molybdenum sulfide catalyst depends on the amount of Mo on the used support. In the present work, we intend to find the optimum Mo loading on CNTs which displays the highest activity and selectivity for HAS.

EXPERIMENTAL SECTION

Preparation of catalysts

Multi wall CNTs (purity >95%) were used as support for preparation of the catalysts. Prior to impregnation the support was treated with 30% HNO_3 reflux at 120˚C overnight, washed with distilled water several times and dried at 120˚C for 6h. All the catalysts were prepared by the incipient wetness impregnation with aqueous solutions of $(NH_4)6Mo_7O_{24}.4H_2O$ and K_2CO_3. First, the support was impregnated with Mo precursor, followed by drying at 120˚C for 2h and calcination in argon flow of 50 mL/min for 4h at 300˚C at a heating rate of 10˚C/min. Then it was impregnated with an aqueous solution of K_2CO_3, dried at 120˚C for 2h and calcined in argon flow of 50 mL/min for 12h at 450˚C at a heating rate of 10˚C/min [16, 21-23]. Six catalysts were prepared with Mo loadings of 5, 10, 15, 20, 25 and 30 wt.% fixing K at 8 wt.%.

ICP-OES

The metal loadings were determined using Varian VISTA-MPX inductively coupled plasma-optical emission spectrometry (ICP-OES) instrument.

BET surface area measurements / BJH pore size distributions

Surface area, pore volume and average pore diameter of the samples were measured using an ASAP-2010 V2 Micrometrics system. The samples were degassed at 200˚C for 4h under 50 mTorr vacuums and their BET area, pore volume and pore diameter were measured.

X-Ray Diffraction (XRD)

The phases and particle sizes of the crystals, present in the catalysts, were analyzed by XRD using a Philips Analytical X-ray diffractometer (XPert MPD) with monochromatized Co/Kα radiation, 2θ angles from 20˚ to 80˚. The Debye–Scherer formula ($d = 0.9\lambda/\beta\cos\theta$, where β is FWHM (Full Width at Half Maximum), λ is wave length of X-ray, 0.9 is a constant) was applied to MoO_3 peaks at $2\theta = 43.3$, in order to calculate the average particle sizes.

Transmission Electron Microscopy (TEM)

The morphology of the support and catalysts was studied by Transmission Electron Microscopy (TEM). Sample specimens for TEM studies were prepared by ultrasonic dispersion of the catalysts in ethanol and the suspensions were dropped onto a carbon-coated copper grid. TEM were carried out using a Philips CM20 (100 kV) transmission electron microscope equipped with a NARON energy-dispersive spectrometer with a germanium detector.

Temperature Programmed Reduction (TPR)

The H_2-TPRs of the catalysts were performed to study the reducibility of the metal species in the catalysts. The calcined catalyst sample (0.05 g) was first purged in a flow of Helium at 140˚C to remove traces of water and gases existed in the catalyst, and then cooled to 40˚C. Then the TPR of each sample was performed using 5% H_2 in Ar stream at a flow rate of 40 mL/min at atmospheric pressure using Micrometrics TPD-TPR 2900 analyzer equipped with a Thermal Conductivity Detector (TCD), heating at a linearly programmed rate of 10˚C/min up to 850˚C.

Hydrogen chemisorption

The amount of chemisorbed hydrogen was measured using the Micrometrics TPD-TPR 2900 analyzer system. 0.2 g of the calcined catalyst was first purged in a flow

Table 1: Textural properties of the fresh and purified carbon nanotubes.

Sample	BET surface area (m^2/g)	Total pore volume (mL/g)	Average pore diameter (Å)	% Metal
Fresh CNTs	209.01	0.48	91.62	0.60%
Treated CNTs	252.59	0.59	94.12	0%

of argon at 140 °C to remove traces of water. The temperature was then raised to 500°C at a rate of 10°C/min and catalyst was reduced for 12 h under H_2 flow and then cooled to 40 °C. Then the flow of H_2 was switched to the argon for 30 min. Afterwards the Temperature Programmed Desorption (TPD) of the samples was performed by increasing the temperature of the samples, with a ramp rate of 40°C/min, to 500°C under the argon flow. The TPD spectrum was used to determine the molybdenum dispersion and its average crystallite size [16].

Reaction setup and experimental procedure

Higher alcohol synthesis had been performed in a fixed-bed reactor system. The reactor was made up of Inconel tubes with of 450-mm length and 22-mm inside diameter. The reactor temperature was controlled via a PID temperature controller. Brooks 5850 mass flow controllers were used to add H_2 and CO at the desired rate to the reactor. The reactor was filled with 0.5g of catalyst diluted with 90-mesh size silicon carbide and housed in a melted salt. The reactor was pressurized to 30 bars with He and the reduction as well as the sulfurization was carried out for 6 h at 450°C at a heating rate of 2°C/min using gas mixture containing 5 mol% H_2S in H_2 and flow rate of 50 mL/min. The temperature was then lowered to the reaction temperature, and the system was pressurized to the reaction condition. The feed gas mixture (H_2/CO ratio of 2) was passed through mass flow controllers and the HAS reaction was carried out at 320°C, 70 bars, and Gas Hourly Space Velocity (GHSV) of 3.6 mL/g catal./h over a period of 24h. The product gas was cooled to 0°C and separated into gas and liquid phases at the reaction pressure. The CO, CO_2 and other gaseous products were monitored with time intervals of 1h. The products were collected after completion of the run and analyzed by means of three gas chromatographs, a Shimadzu 4C gas chromatograph equipped with two subsequent connected packed columns; Porapak Q and molecular sieve 5Å and a Thermal Conductivity Detector(TCD) with argon which was used as a carrier gas for hydrogen analysis. A Varian CP 3800 with a chromosorb column and a thermal conductivity detector were used for CO, CO_2, CH_4 and other non-condensable gases. The Varian CP 3800 with a Petrocol Tm DH100 fused silica capillary column and a flame ionization detector were used for analysis of organic liquid products so that a complete product distribution could be provided.

RESULTS AND DISCUSSION

3.1. Characterization

Textural properties of the fresh and purified carbon nanotubes are given in the Table 1. The data indicates that in the case of acid-washed support, surface area, total pore volume and average internal diameter of nanotubes increased significantly which will result in better dispersion of metal as well as enhancement of catalyst activity. Table 1 also shows the metal (Fe) content for the untreated fresh CNTs and acid treated CNTs (determined by ICP). As shown, the amount of encapsulated metal content in the fresh CNTs was about 0.6wt% which was decreased to zero for acid treated CNTs. Results of surface area measurements for the catalysts are given in the Table 2. These results show that the BET area of the 15% loaded Mo and 8% loaded K catalyst on 252.59 m^2/g CNTs is 136.1 m^2/g. A 15wt.% loading of metal is equivalent to 22.5% by weight MoO_3 and a 8wt.% of K loading is equivalent to 9.6% by weight K_2O . Since, the CNTs are the only contributor to the area, and then the area of the 15Mo8K/CNTs catalyst should be approximately 0.679× 252.59 = 171.51 m^2/g. However, the value is somewhat lower, which indicates some pore blockage by metal oxide clusters in the CNTs supported catalyst. Calculations and the measured values on Table 2 show that the pore blockage increases up on increasing the Mo loadings to 30 wt.%. The elemental compositions of the catalysts are given in Table 3. The measured values for the prepared catalysts are found to be slightly lower compared to the targeted values. The discrepancies may be due to incomplete impregnation of Mo, because of the

Table 2: Textural properties of the catalysts.

Sample	BET surface area (m^2/g)	Total pore volume (mL/g)	Average pore diameter (Å)
5Mo8K/CNTs	191.3	0.46	124
10Mo8K/CNTs	152.5	0.44	127
15Mo8K/CNTs	136.1	0.42	129
20Mo8K/CNTs	127.4	0.40	132
25Mo8K/CNTs	106.0	0.36	139
30Mo8K/CNTs	84.3	0.33	143

Table 3: Chemical composition of CNTs supported catalysts.

Catalyst	Targeted composition (wt.%)		Measured composition (wt.%)	
	Mo	K	Mo	K
5Mo8K/CNTs	5	8	4.9	7.9
10Mo8K/CNTs	10	8	9.7	7.9
15Mo8K/CNTs	15	8	14.4	7.9
20Mo8K/CNTs	20	8	19.2	7.9
25Mo8K/CNTs	25	8	24.2	7.9
30Mo8K/CNTs	30	8	28.6	7.9

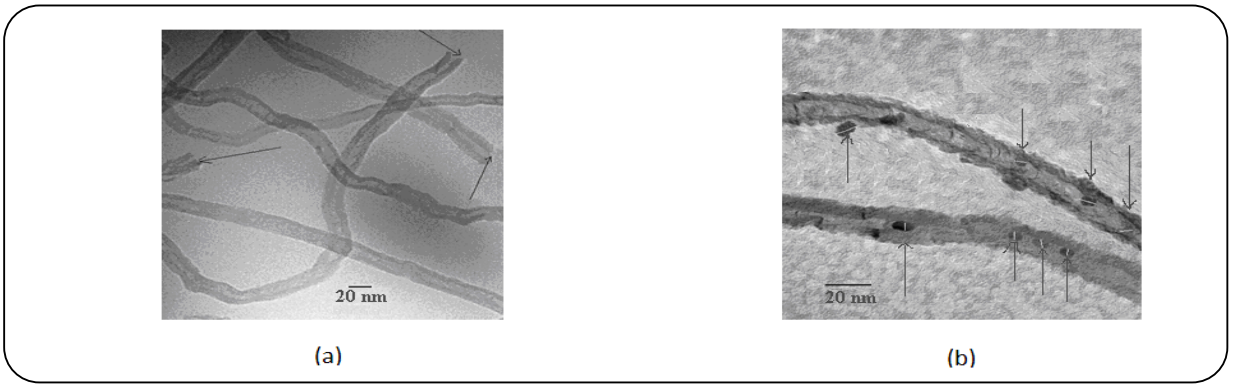

Fig. 1: (a) TEM image of purified CNTs (b) TEM image of 15Mo8K/CNTs catalyst.

hygroscopic nature of the Mo precursor. Fig. 1a and 1b present the TEM images of the purified support and 15Mo8K/CNTs catalyst respectively. TEM image of 15Mo8K/CNTs catalyst shows that the particles are distributed both inside and outside of the nanotube walls. The sizes are of particles located inside the nanotubes in the range of 3-9 nm. However particles located outside the nanotubes have grown to about 16 nm. It seems that the CNTs' channels have restricted the growth of the particles inside the tubes. Fig. 2 depicts the size distribution of the particles, which is determined using the population of the total particles of the catalyst based on data taken from 5 TEM pictures. According to this figure, the average particle size for the 15Mo8K/CNTs catalyst is 7.1 nm. Fig. 3 presents XRD pattern of the catalysts with different loadings of molybdenum. As shown, increasing the amount of Mo from 5 to 30 wt.% increases intensity of the peaks corresponding to MoO_3 (peaks at 2θ values of 43.3, 63.2 and 71.9), indicating the grown particle size of MoO_3 at higher metal loadings [13,16-18]. Table 3 shows the average sizes of MoO_3 particles calculated from the XRD patterns, using

the Debye-Scherer formula at 2θ value of 43.3. As can be seen increase in Mo loading from 5 to 30wt.% increases the crystal diameter of MoO_3 from 4.1 to 16.4 nm. Also, three peaks at 2θ values of 25.8, 31.3, 40.4, and 46.3 with weak intensities can be correspond to the crystalline structure of K–Mo-O mixed oxide species ($K_2Mo_2O_7$, K_2MoO_4, $K_2Mo_7O_{20}$, KMo_4O_6, and $K_{0.33}MoO_3$) [13,16-18]. When Mo loading increases from 5 to 15 wt.%, the corresponding K–Mo-O peaks appear more significantly. This implies that with increase in Mo loading to 15 wt.%, the chemical interactions between K–Mo–O species are increased, enhancing the conditions for the formation of alcohols [18]. However, increasing Mo loadings to 30 wt.% decreases the intensity of the peaks which is corresponding to K–Mo-O mixed oxide species. This shows that the K/Mo ratio of about 0.5 is the best state for the formation of K-Mo-O mixed oxides [19].

Fig. 4 shows Temperature Programmed Reduction (TPR) diagrams of the catalysts containing different amounts of Mo and 8 wt.% K. The first peak in the TPR spectrum of the catalysts is typically assigned to the reduction of Mo^{6+} to Mo^{4+}. The second peak is mainly assigned to the second reduction step, which is mainly reduction of Mo^{4+} to metallic Mo^o [16]. Increasing Mo from 5% to 15wt.% decreases temperature of first peak temperature from 518 to 504˚C although the second peak temperature increases from 782 to 804˚C. This is due to the fact that increasing Mo loading to 15wt.% promote the formation of Mo-K mixed oxides species (As shown by XRD) that are reducible at lower temperatures. When Mo loading increases from 15 to 30wt.% the decrease in the first TRP peak is negligible. However, second TPR peak temperature increases to 825°C, indicating that increased Mo addition inhibited the reduction of catalysts supported on CNTs (Molybdenum is in form of MoO_3). It is notable that with increasing Mo loadings, H_2 consumption which is proportional to the percentage of catalyst reduction increases from 2.04 to7.64 mmol H_2/g cat. then levels off. The maximum H_2 consumption occurs in 20wt.% Mo loadings.

The results of hydrogen chemisorption tests are given in Table 5. As shown, increased Mo loading from 5 to 20wt.%, increased the hydrogen uptake which decreased when the Mo loading is further increased to 30wt.%. This shows that some of the pores are blocked by increasing the Mo to 30wt.%. Percentage dispersion, decreased from

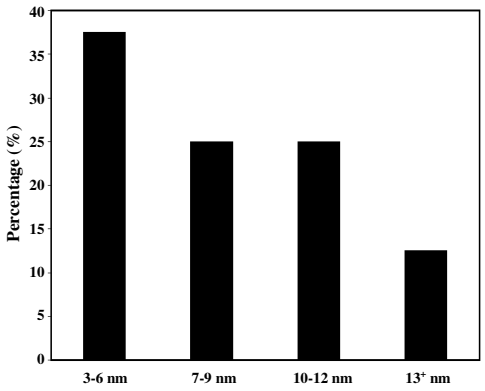

Fig. 2: Particle size distribution for 15Mo8K/CNTs catalyst.

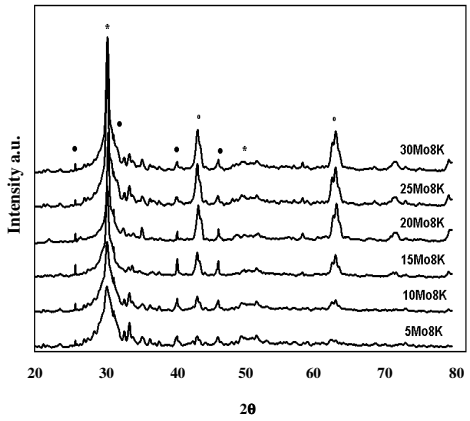

Fig. 3: XRD patterns of the calcined catalysts with different Mo loadings (•; K-Mo-O, *; CNTs, o; MoO_3).

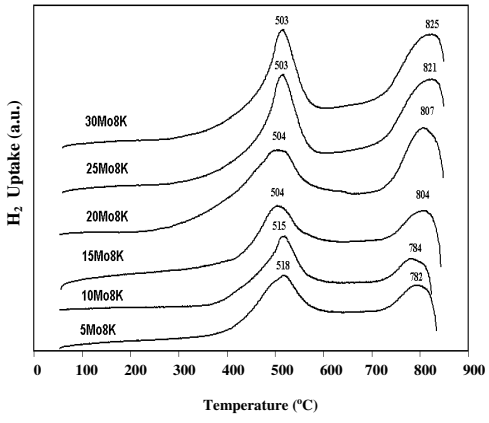

Fig. 4: TPR profiles for the catalysts with different Mo loadings.

Table 4: Average particle size for the catalysts (determined by XRD).

Catalyst	dp (nm) (determined by XRD)
5Mo8K/CNTs	4.1
10Mo8K/CNTs	5.4
15Mo8K/CNTs	7.5
20Mo8K/CNTs	9.1
25Mo8K2Co/CNTs	12.8
30Mo8K4Co/CNTs	16.4

Table 5: H_2 chemisorption results for the catalysts.

Catalyst	μ mole H_2 desorbed/ g. cat	% Dispersion	dP (nm)
5Mo8K/CNTs	199	76.4	4.5
10Mo8K/CNTs	346	66.4	5.5
15Mo8K/CNTs	399	51.1	7.5
20Mo8K/CNTs	459	44.1	9.2
25Mo8K/CNTs	432	33.2	12.9
30Mo8K/CNTs	421	26.9	16.7

76.4 to 26.9 upon increasing Mo from 5 to 30wt.%. The particle diameter increased, which is in agreement with the results of XRD tests. Higher dispersion and small molybdenum cluster sizes will increase the number of sites available for CO conversion reactions in CNTs supported molybdenum catalysts.

Activity and products selectivities

Synthesis of higher alcohols was carried out after reduction and sulfidation of catalysts in a fixed bed reactor at 320°C, 70 bars, GHSV of 1.714 h^{-1} and H_2/CO=2. The liquid products were collected at 0°C and the outlet gas was analyzed to measure the CO conversion. The analysis of liquid indicates that methanol, ethanol, and n-propanol are the major products together with small amounts of higher alcohols. The analysis of outlete gas indicates that methane is the major component apart from CO, H_2 and CO_2.

Fig. 5 presents the H_2 and CO conversion variations for the catalysts with different Mo loadings. This figure reveals that with increasing the amount of Mo loading, the CO and H_2 conversions show a remarkable increase, passes through a maximum at Mo loading of 20wt.% and then starts to decrease. Comparing the data of this figure with the data of Table 5 demonstrate that the %CO conversion increases in accordance with the hydrogen uptake, with addition of molybdenum loading up to 20 wt.%, and then starts to decrease. The catalyst with 20wt.% Mo and 8wt.% K showed the highest CO conversion of 31.5% and H_2 conversion of 27.2%. It can be concluded that increasing Mo loadings from 5 to 20 wt.% increases the active surface area of the catalysts which in turn leads to enhancement of CO and H_2 conversions. Also the increase in % CO and H_2 conversions upon increasing Mo loadings from 5 to 20 wt.% can be due to the enhancement in reduction of Mo^{6+} to metallic Mo^{4+}. So, in feed conversion point of view, this value is a proper loading when CNTs with about 250 m^2/g surface area and 0.6 void fractions is the catalyst support. Fig. 6 shows variations in selectivity of alcohols and hydrocarbons in liquid products with %Mo loadings. Although catalyst with 20 wt.% Mo showed the highest conversion (Fig. 5), catalyst with 15 wt.% Mo and 8 wt.% K showed highest selectivity towards higher alcohols. On increasing Mo content from 5 to 15 wt.%, the alcohols selectivity is increased from 34.4 to 45.3%, and decreased to a value of 31.9% upon increasing Mo loading to 30 wt.%. It has been suggested that sulfidation of the mixed oxides

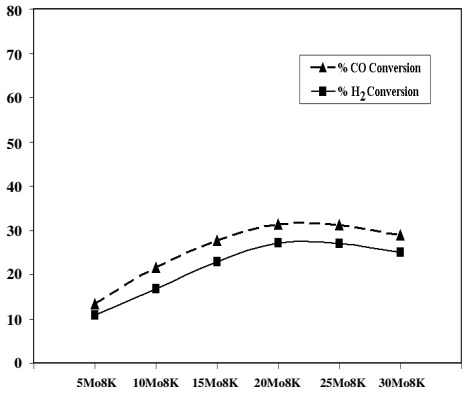

Fig. 5: Percentage H_2 and CO conversion variations with different Mo loadings.

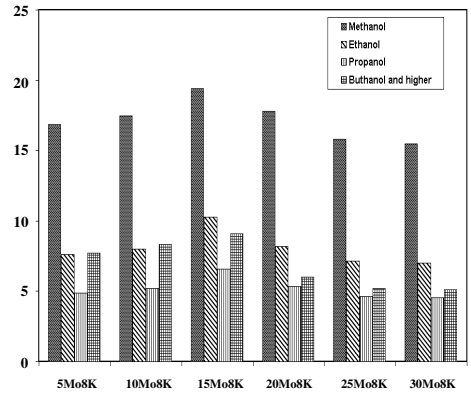

Fig. 7: Variations in the selectivity trends of individual alcohols with %Mo loadings.

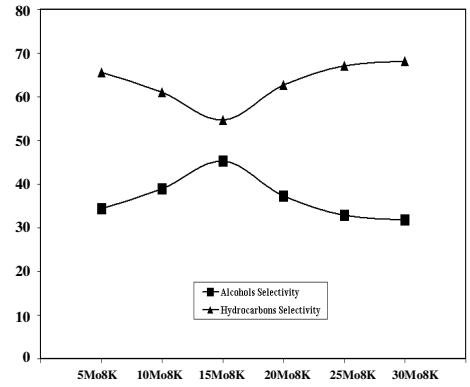

Fig. 6: Variations in the selectivity of alcohols and hydrocarbons in liquid products with %Mo loadings.

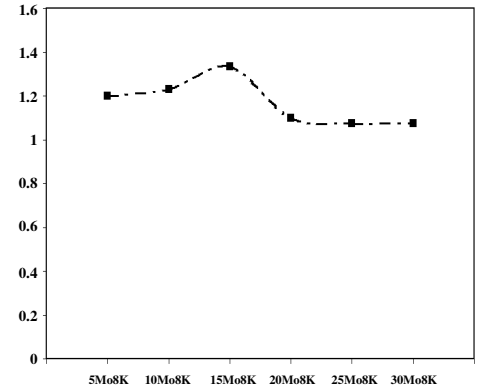

Fig. 8: Variations of HA/CH_3OH ratio with %Mo loadings.

present in calcined form of the catalysts and formation of the Mo-K-S species like K_2MoS_4 are responsible for increasing the alcohol formation [16-18]. Our XRD results showed that on increasing Mo loading from 5 to 15wt.% the intensity of the peaks corresponding to Mo-K-O mixed oxides increased and the intensity of the said peaks decreased upon increasing Mo loading from 15 to 30wt.%. These interactions are responsible for the formation of ethanol and higher alcohols via flowing CO insertion mechanism [20].

$$CO + 2H_2 \leftrightarrow CH_3OH \quad (1)$$

$$CH_3OH + H_2 \rightarrow CH_4 + H_2O \quad (2)$$

$$CH_3OH + CO + 2H_2 \rightarrow C_2H_5OH + H_2O \quad (3)$$

$$C2H_5OH + CO + 2H_2 \rightarrow C_3H_7OH + H_2O \quad (4)$$

$$CO + H_2O \leftrightarrow CO_2 + H_2 \quad (5)$$

The increase in HC selectivity is observed with increased Mo, which may be due to increased availability of hydrogenation centers, i.e. MoS_2 species as also confirmed by XRD results. Fig. 7 shows the selectivity trends of individual alcohols with increased Mo loadings. The maximum HA of 22.5% is observed over 15Mo8K/CNTs. The reason may be better explained from the XRD and TPD tests. It is clear from XRD and TPD that the catalysts with 20, 25 and 30wt.% Mo showed large MoO_3 particle size, which is responsible for poor activity of these catalysts towards the formation of HA. Fig. 8 shows the variations of HA/CH_3OH with increased

Mo loadings. The catalyst with 15 wt.% Mo and 8 wt.% K shows highest ratio of HA production rate to methanol production rate. Consequently, in HA selectivity point of view, 15 wt.% Mo is the suitable loading when CNTs are the catalyst supports.

CONCLUSIONS

Cobalt promoted alkalized MoO_3 supported on CNTs catalyst is used to produce higher alcohols from syngas. From the TEM images, it was found that metal species were uniformly distributed inside and outside of the tubes, with particle sizes in the range of 3 to 16 nm. Among the catalysts with different Mo loadings supported on CNTs, catalyst with 20 wt.% Mo and 8 wt.% K showed the highest CO and H_2 conversions. However the total alcohol selectivity reached a maximum of 45.3 wt.% on the catalyst with 15 wt.% Mo and 8 wt.% K. The catalyst with 15 wt.% Mo exhibited selectivity of 35.3 wt.% towards HA alcohols.

Received : Aug. 25, 2011 ; Accepted : Apr. 14, 2012

REFERENCES

[1] Herman R., "Studies in Surface and Catalyst'', (Chapter 7), Elsevier, Amsterdam, (1990).

[2] Natta G., Colombo U., Pasquon I., "Catalysis", Emmet P.H. (Ed.) Vol. 5, (1957).

[3] Morgan G.T., Hardy D.V.N., Procter R.A., Physics and Chemistry of Alkali Metal Adsorption, *J. Soc. Chem. Ind. Trans.*, **1T**, p. 56 (1932).

[4] Smith K.J., Anderson R.B., Alcohols Synthesis Using Modified Methanol Synthesis Catalysts, *Canadian Journal of Chemistry Engineering,* **61**, p. 40 (1983).

[5] Smith K., Anderson R., Mechanism of Ethanol Formation, *J. Catalysis*, **85**, p. 428 (1984).

[6] Quarderer Q.J., Cochram G.A., Catalytic Process for Producing Mixed Alcohols from Hydrogen and Carbon Monoxide, PCT *Int. Pat. Publication No. WO84/03696* (1984).

[7] Kinkade N.E., Process for Producing Alcohols from Carbon Monoxide and Hydrogen Using an Alkali-Molybdenum Sulfide Catalyst, PCT *Int. Pat. Publication No. WO 85/03073* (1985).

[8] Jackson G.R., Mahajan D., Method for Production of Mixed Alcohols from Synthesis Gas, *U.S. Patent 6,248,796* (2001).

[9] Chaumette P., Courty P., Durand D., Grandvallet P., Travers C., Process for Synthesizing a Mixture of Primary Alcohols from a Synthesis Gas in the Presence of a Catalyst Containing Copper, Cobalt, Zinc, and Aluminum, *GB Patent, 2,158,730* (1985).

[10] Woo H., Park K.Y., Mixed Alcohol Using Mo_2C Catalysts, *Appl. Catal.*, **75**, p. 267 (1991).

[11] Jiang M., Bian G.Z., Fu Y.L., The Structure of Oxidic and Sulfided Mo Catalysts Upported on AC Was Studied by Means of X-Ray Diffraction, *Journal of Catalysis*, **146**, p. 144 (1994).

[12] Lee J.S., Kim S., Lee K.H., Nam I.S., Kim Y.G., Woo H.C., Effect of K-Mo Interaction in K-MoO_3/ γ-Al_2O_3 on the Properties for AS from Syngas, *Appl. Catal.*, **110**, p. 11(1994).

[13] Tatsumi T., Muramatsu A., Tominga H., Mechanistic Study on the AS Over Mo Catalysts: Addition of Probe Molecules to CO-H_2, *Journal of Catalysis*, **115**, p. 388 (1989).

[14] Iranmahboob J., Toghiani H., Hill D., Dispersion of Alkali on the Surface of Co-MoS_2: A Comparison of K and Cs as a Promoter for HAS, *Appl. Catal.*, **247**, p. 207 (2003).

[15] Iranmahboob J., Hill D.O., Alcohol Synthesis from Syngas over K_2CO_3/CoS/MoS_2 on Activated Carbon, *Catalysis Letters*, **78**(4) p. 49 (2002).

[16] Surisetty V., Tavasoli A., Dalai A., Synthesis of Higher Alcohols from Syngas over Alkali Promoted MoS_2 Catalysts, *App. Catal.*, **365**, p. 43 (2009).

[17] Li Z., Fu Y.L., Bao J., Jiang M., Hu T.D., Liu T ., Xie Y.N., Effect of Cobalt Promoter on Co-Mo-K/C Catalysts Used for Mixed Alcohol Synthesis, *Applied Catalysis*, **220**, p. 21(2001).

[18] van Berge P.J., van de Loosdrecht J., Barradas S., van der Kraan A.M., Oxidation of Cobalt Based F.T. Catalysts as a Deactivation Mechanism, *Catalysis Today*, **58**, p. 321 (2000).

[19] Xiaoming M., Guodong L., Hongbin Z., Co-Mo-K Sulfide-Based Catalyst Promoted Bymulti-Walled CNTs for Higher Alcohol Synthesis, *Chinese J. Catal.*, **27**, p. 1019 (2006).

[20] Santiesteban J., Bogdan C.E., Higher Alcohols Synthesis Using Mobased Catalysts, Proceedings of 9th ICC, 2, Calgary, Canada, p. 561 (1988).

[21] Surisetty V., Dalai A., Kozinski J., Intrinsic Reaction Kinetics of HAS from Syngas over a Alkalized Co-Rh-Mo Catalyst Supported on MWCNTs, *Energy Fuels,* **24**, p.4130 (2010).

[22] Surisetty V., Dalai A., Kozinski J., Influence of Porous Characteristics of the Support on Alkali-Modified Co-Rh-Mo Sulfided Catalysts for HAS, *Appl. Catal,* **393**, p. 50 (2011).

[23] Surisetty V., Dalai A., Kozinski J., Effect of Rh on MWCNT-supported Alkali-modified MoS_2 for HAS from CO Hydrogenation" *Appl. Catal.,* **381**, p. 282 (2010).